



ChemTech

## International Journal of ChemTech Research

CODEN (USA): IJCRGG ISSN: 0974-4290  
Vol.7, No.3, pp 1529-1536, 2014-2015

ICONN 2015 [4<sup>th</sup> - 6<sup>th</sup> Feb 2015]

International Conference on Nanoscience and Nanotechnology-2015  
SRM University, Chennai, India

### Effect of External Magnetic Field on Morphology, Structural and Magnetic Property of Nickel Nanostructures

Anuraj Sundararaj<sup>1\*</sup>, Mahdiyari Bagheri<sup>1</sup>, Gopalakrishnan Chandrasekar<sup>1</sup>,  
Tejabhram Yadavalli<sup>1</sup>, Helen Annal Therese<sup>1</sup> and Karthigeyan Annamalai<sup>2</sup>

<sup>1</sup>Nanotechnology Research Center, SRM University, Chennai, Tamilnadu, India.

<sup>2</sup>Department of Physics and Nanotechnology, SRM University,  
Chennai, Tamilnadu, India.

**Abstract :** Nickel nanostructures were synthesized using wet chemical synthesis technique in the presence of manifold external magnetic field. Nickel chloride and hydrazine hydrate were used as the precursor and reducing agent, respectively. The reactions were performed in external magnetic field of 0 gauss to 1200 gauss with an interval of 200 gauss for each reaction. It was observed that the synthesized Ni nanostructures were face centered cubic with dominant [111] orientation. The morphology of nanostructures was observed to change with change in external magnetic field. Nickel nanofibers with an average diameter of 52 nm and average length of 375 nm were found in the 800 Gauss sample. Vibrating sample magnetometer studies performed on selected samples indicated significant change in saturation magnetization and coercivity of the nanofibers, with respect to the external magnetic field used. The yields obtained from all experiments were found to be stable for three months when kept at normal atmospheric conditions.

**Keywords:** External Magnetic Field, Morphology, Structural and Magnetic Property, Nickel Nanostructures.

#### Introduction

Nickel nanostructures are used in many applications such as chemical catalysis<sup>1</sup>, medical diagnostics and treatment techniques like magnetic resonance imaging and magnetic hyperthermia<sup>2</sup>, magnetic data storage devices<sup>3</sup>, boundary layer capacitors (BLC), multilayer ceramic capacitors (MLCC)<sup>4, 5, 6</sup>, surface enhancement coatings and environmental remediation. There are many methods to synthesize nickel nanostructures by chemical and physical means. Wet chemical reduction process<sup>7</sup>, polyol process<sup>8</sup>, chemical vapor deposition (CVD)<sup>9</sup>, physical vapor deposition (PVD)<sup>10</sup>, molecular beam epitaxy (MBE)<sup>11</sup>, ball milling<sup>12</sup> and electro spinning<sup>13</sup> are some of the techniques often used. Among the above mentioned methods, the wet chemical method is simpler and cost effective.

In wet chemical methods, the use of extrinsic factors such as temperature, pressure, pH and concentration as parameters to control the growth of nanostructures has been studied extensively in the past<sup>14, 15, 16</sup>. Nickel fibers have also been synthesized by template based methods for the fabrication of arrays of

nickel fibers on tin doped indium oxide substrates by randomization and electrodeposition<sup>17</sup> and polyaniline based templates on alumina substrates<sup>16</sup>. The use of external magnetic field to attain control over the morphology of nickel nanoparticle is of major interest due to its ability to provide control over the morphology of magnetic nanoparticle without any capping agents. The use of a magnetic field for the fabrication of oriented magnetic structures using electron beam assisted physical vapor deposition in the presence of magnetic field has been discussed in our earlier paper<sup>18</sup>.

The effect of external magnetic field on conventional template free wet chemical synthesis of magnetic particles has also been done in order to understand the role of magnetic field with respect to the structure of the magnetic particles<sup>19,20,21,22</sup>. The magnetic field used in these experiments has been always over 600 Gauss and they are not systematically performed over a range such as 0 -1200 Gauss<sup>19-22</sup>. Hence a comprehensive study of the effect of magnetic field in the range (0-1200 G) is essential to understand the influence of an external magnetic field. In this paper, we have discussed the influence of an *in situ* external magnetic field; in the range of 0 – 1200 Gauss, on the morphological and magnetic properties of nickel nanostructures.

Hydrazine hydrate was chosen as a weak reducing agent since it provides enough time for nickel nanofibers to form and hydrazine hydrate reduction is one of the most convenient methods for the synthesis of nickel nanoparticles<sup>14,15</sup>. The external magnetic field was varied from 0 – 1200 Gauss at an interval of 200 Gauss for each experiment. As nickel is ferromagnetic in nature, an effect of external magnetic field on the morphology of the synthesized nickel nanoparticles was expected.

## Experimental

### Materials

Analytical grade nickel chloride hexahydrate [NiCl<sub>2</sub>·6H<sub>2</sub>O], acquired from Loba Chemie, analytical grade hydrazine hydrate [N<sub>2</sub>H<sub>4</sub>·H<sub>2</sub>O] and acetone [CH<sub>3</sub>COCH<sub>3</sub>], acquired from Rankem, sodium hydroxide [NaOH] and sodium borohydride (NaBH<sub>4</sub>) acquired from SISCO Research Laboratories were used. Millipore deionized water was used as the solvent in all the reactions.

### Experimental setup

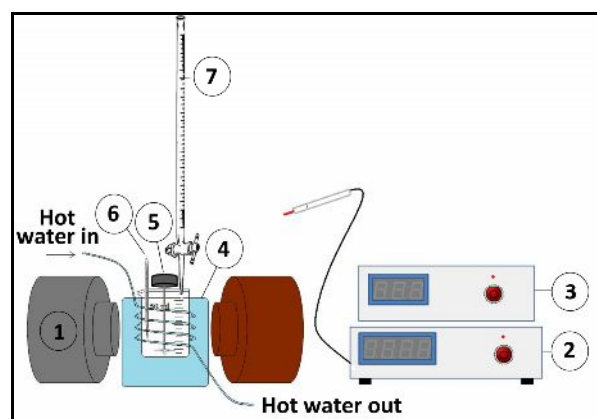


Fig.1. Customized Experimental setup depicting the different parts of the experimental setup

A custom made temperature controlled reaction setup was placed between the poles of electromagnets (Fig.1). Digital thermometer and gauss meter were used to measure temperature and magnetic flux density, respectively.

### Nickel nanostructure synthesis

In the wet chemical synthesis process, reduction of the precursor by strong reducing agents like NaBH<sub>4</sub> is known for its larger and quicker yield. Vigorous reactions due to strong reducing agents usually lead to agglomeration of the yield and results in larger particle sizes and non linearity in their dimensions. Employing weaker reducing agents reduces swift congestion of metal ions around each nucleating center thereby reduces agglomeration. Experiments were divided into fast and slow reactions, performed by employing NaBH<sub>4</sub> and hydrazine hydrate respectively as reducing agents.

In the fast reactions 10 ml of 0.4 M Nickel Chloride precursor solution and 10 ml of 0.8 M sodium borohydride solution was prepared. The nickel chloride precursor was titrated into the beaker containing Sodium Borohydride for half an hour. The solution in the beaker turned into a dark black precipitate. The yield was then washed multiple times and dried at 80 °C for 48 hrs yielding black nickel powder. The reactions were performed in the presence of an external magnetic field; the intensity of which was increased from 0 Gauss to 1200 Gauss with an interval of 200 Gauss. The black precipitate obtained from all reactions were washed multiple times and dried at 80 °C for 48 hrs, yielding black nickel powder.

In the slow reactions, 10 ml of 0.4 M nickel chloride precursor solution was prepared. 10 ml of pH 12 sodium hydroxide solution was mixed with 10 ml of hydrazine hydrate to prepare a reducing solution. The as-prepared reducing agent was then taken into a 50 ml beaker and stabilized at 60 °C followed by slow titration of precursor into the beaker. A faint blue solution was formed followed by a purple precipitate, which then finally transformed into a shining black precipitate. Experiments were carried out by varying the magnetic field from 0 Gauss to 1200 Gauss with intervals of 200 Gauss. The obtained shiny black precipitate from all the reactions were then washed multiple times and dried at 80 °C for 48 hrs yielding fine shining black pure nickel powder.

### Characterization

The crystallinity and phase purity of the nickel nanoparticles were studied using Panalytical X'pert Pro x-ray diffractometer (XRD), fitted with a graphite monochromator. The diffraction patterns were measured at 45 kV tension, 40 mA current with a 0.02° step size with 2θ ranging from 10°-160° (Fig.2). The morphology of the nanostructures was studied using FEI's Quanta 200 FEG field emission scanning electron microscope (FESEM). The magnetic property was examined by Lakeshore 7410 vibrating sample magnetometer (VSM) with a maximum magnetizing field of 3 Tesla.

## Results and Discussion

### Reaction mechanism for nickel formation

#### Sodium Borohydride reduction (Fast reaction)

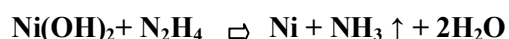
Sodium borohydride is a pseudo-stable compound that disintegrates to give hydrogen radical that reduces the precursor material.



The nickel chloride precursor solution was reduced using sodium borohydride solution. The solution yielded dark black precipitate. The yield was later found to be black amorphous nickel nanoparticles.

#### Hydrazine hydrate reduction (Slow reaction)

Hydrazine is a dibasic reducing agent with oxygen scavenging property at elevated temperatures or in the presence of a catalyst. This property effectively reduces a metal precursor into its pure metallic component.



In the above reaction, the role of sodium hydroxide is to maintain optimum pH level while the heating source provides the necessary activation energy for the hydrazine hydrate to start reacting with the precursor solution.

When the precursor is titrated into a pH 12 reducing solution, the mixture turns pale blue. As the reaction proceeds, the solution turns into a purple precipitate which indicates the formation of nickel hydroxide. The reaction ends with shiny, black precipitate formed at the bottom of the beaker confirming the formation of nickel. The nickel nanoparticles were found to deposit on the walls of the beaker, giving it a shiny mirror like appearance. The importance of using hydrazine hydrate as the reducing agent instead of other stronger reducing agents such as sodium borohydride was realized after certain experimental trials which showed that the particles were big spherical amorphous microstructures. The borohydride reaction is significantly faster than the aforementioned hydrazine hydrate reaction. Thus, the reaction time of the borohydride reduction is insufficient for the particles to be influenced by the external magnetic field. This along with the formation of nickel boride<sup>11</sup>, which is diamagnetic in nature, inhibits the influence of the external magnetic field on fabricated

nanostructures. This provides an insight into the importance of choosing the right reducing agent to understand the influence of external magnetic field on the nickel nanostructures.

### X-Ray Diffraction results

XRD analysis was performed on both the fast reactions and slow reactions. The results from the fast reactions (Fig.2) gave a diffractogram with no peculiar peaks. This indicates that the samples are amorphous. Here the amorphous nature of the synthesized nanopowder can be attributed to the formation of nickel boride compounds rather than pure nickel. It has been discussed by *T.S.N. Sankara Narayanan et al*, [16] that the formation of nickel boride disrupts the nickel nucleation due to large boron segregation.

Fig.2 (inset) shows the XRD patterns of the hydrazine hydrate synthesis of the samples in the presence of various magnetic fields. The graph shows distinct peaks corresponding to  $2\theta$  values  $44.48^\circ$ ,  $51.832^\circ$  &  $76.352^\circ$ . These peak positions can be attributed to the presence of FCC nickel (JCPDS# 70-1849). The  $2\theta$  values  $44.48^\circ$ ,  $51.832^\circ$  &  $76.352^\circ$ , corresponds to nickel with [111], [200] and [220] planes respectively, with [111] being the dominating plane. One can also observe no changes in the peaks positions and the intensities with respect to change in the intensity of the applied magnetic field. This confirms that there is no influence of the magnetic field on the crystal structure of the nickel nanostructures.

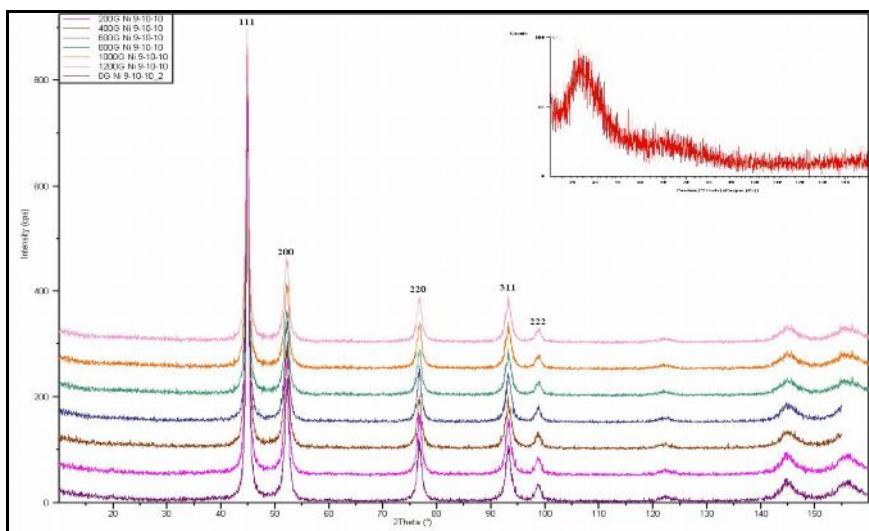


**Fig.2. (a) The amorphous XRD pattern of the fast reaction and (b) Comparative XRD pattern of the yields obtained from 0, 200, 400, 600, 800, 1000, 1200 Gauss synthesis**

### The effect of external magnetic field on morphology

One of the main focuses of this work was to study the effect of external magnetic field on the morphology of magnetic nickel particles. The SEM analysis was conducted on both the yields of the fast reaction and slow reactions. The images of the yield from the fast reactions (Fig.3) showed the formation of spherical particles randomly spread over the sample. The SEM images did not show any significant variation with change in the magnetic field. The reason for the absence of change in morphology can be attributed to the formation of Ni-B complexes with no inherent magnetic moment. The SEM analysis of the yield obtained from the fast reactions showed no significant change with respect to the external magnetic field.

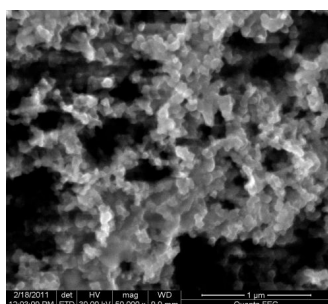


**Fig.3. FESEM images for 800 Gauss reaction with  $\text{NaBH}_4$ .**

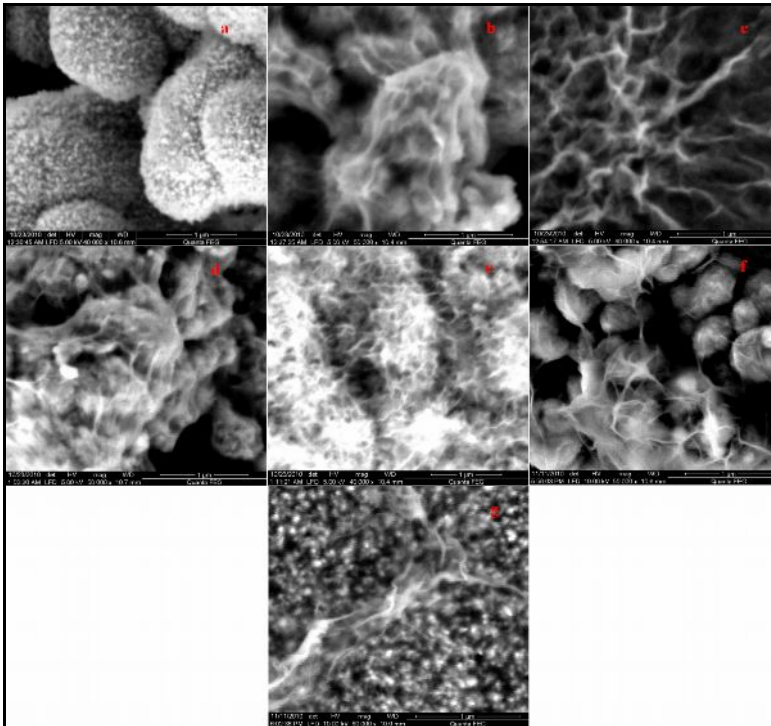


**Fig.4.FESEM images for 0 Gauss -1200 Gauss reaction**

Fig.4a–4g depicts the change in morphology of the yields which were synthesized in the presence of magnetic field at intensities of 0, 200, 400, 600, 800, 1000 and 1200 Gauss, respectively. The SEM analysis of the yields obtained from the slow reactions revealed an interesting phenomenon. There was formation of nanofibers in the samples fabricated in magnetic fields between 800 – 1200 Gauss.

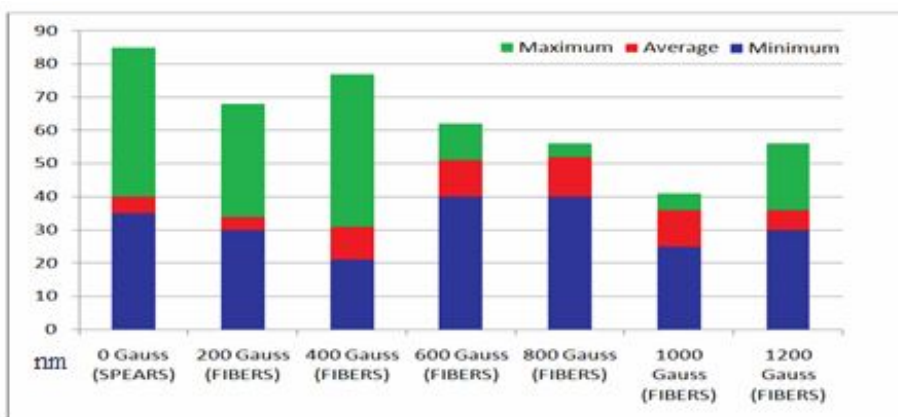


**Fig.5. Graph representing sample diameter of various yield obtained**

FESEM results showed that the sample synthesized in the absence of external magnetic field contained spherical (entropically stable structures) nickel nanoparticles that agglomerated to form spheres of larger sizes (Fig.4a), similar to the previous work reported<sup>20</sup>. The average diameter of the spherical nanoparticles that were formed in this sample was 45 nm which agglomerated into larger spheres, ~1 μm in diameter. The sample synthesized at 200 Gauss (Fig.4b) consists of agglomerated or clusters of spherical nanoparticles. The average diameter of the spherical nanoparticles in this sample was at the range of 20-50 nm in diameter (Fig.5). The FESEM images of samples fabricated with field intensities between 400 – 1200 Gauss revealed an interesting phenomenon. The images show that the nickel formed into 1-D nanofibers (Fig.4c–4f). The dynamics of the formation of the nanofibers can be hypothesized to be a simple nuclei driven growth influenced by the lines of force of the external magnetic field. As in typical wet chemical reactions, the formation of new nuclei takes place continuously in the solution. Under the presence of a strong magnetic field, these nuclei attract nearby nuclei which naturally get aligned due to the restrictive influence of the magnetic lines of force in the solution

as described by Zhang Meng *et al*<sup>12, 19</sup>. This would explain the formation of 1-D nanofibers and the absence of 0-D nanostructures at field intensities above 400 G. The diameter of the fibers thus synthesized remained consistent for all the samples, and ranged between 30 nm – 50 nm. The length of the fibers ranges between 134 nm (Fig.4c) to 990 nm (Fig.4g). The increased length can be understood to be the result of the direct influence of a stronger magnetic field which accentuates the formation of longer nickel fibers as compared to the weaker magnetic fields. The fiber density was also found to vary with varying magnetic fields. These results clearly indicate the significant influence of external magnetic fields on the morphology of the nickel nanoparticles. From the FESEM results, it was evident that the numbers per unit area of nickel nanofibers was the maximum in the 800 G sample.

### The effect of external magnetic field on magnetic property

VSM analysis was performed to compare the magnetic property of the 1-D nanofibers fabricated at 800 G with the sample fabricated in the absence of an external magnetic field (spherical nanostructures). The values are tabulated in Table 1.

VSM analysis was performed on two chosen samples based on the SEM images obtained at room temperature. The sample with the maximum fiber formation (800 Gauss) was chosen as the ideal candidate for comparison of its properties with the control sample (0 Gauss). These samples were chosen in order to understand the change in the magnetic properties of spherical nickel nanoparticles (control) and fully formed nanofibers (800 G).

**Table 1: Magnetic properties of samples synthesized at 0 Gauss and 800 Gauss**

Sample	Average diameter (nm)	Saturation magnetization $M_s$ (emu/g)	Remnant magnetization $M_r$ (emu/g)	coercivity $H_c$ (Oe)
0 Gauss	40	28.74176	10.01323	456.73
800 Gauss	52	55.34814	18.03592	438.27

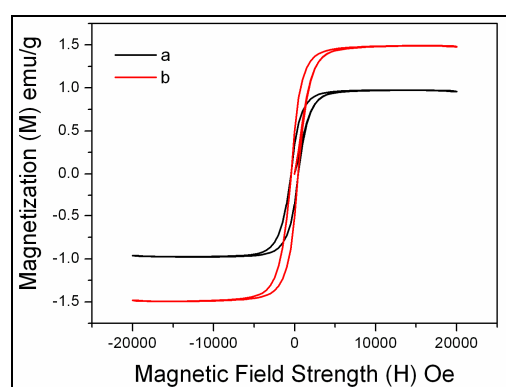


**Fig.6.VSM result for sample synthesized at (a) 0 gauss (b) 800 gauss**

The hysteresis loop (Fig.6) shows that the saturation magnetization and the remnant magnetization of the sample which was synthesized at 800 G were higher than those of the sample synthesized in the absence of an external magnetic field. This can be attributed to influence of shape anisotropy in the samples containing the nanofibers. The large number of randomly oriented nanofibers in the 800 G sample and the presence of an hard and easy axis of magnetization (as expected for 1-D nanofibers) results in the increase in the saturation and remnant magnetizations as compared to the sample fabricated in the absence of a magnetic field, which predominantly consists of 0-D spherical (isotropic) nickel nanostructures. It can also be seen that the coercivity of both the samples were ~similar. Also, the values indicate that the squareness of hysteresis loop<sup>13, 16</sup> is 0.34 for the 0 Gauss sample and 0.32 Gauss for the 800 Gauss sample.

## Conclusion

A study of the external magnetic field as an extrinsic factor in the formation and physical properties of nickel nanostructures was carried out. Nickel nanostructures with definite shape and size were synthesized and characterized. The synthesis procedure was simple, dependable and reproducible. XRD spectrums revealed that the yields of all experiments performed in the presence of 0-1200 Gauss external magnetic field were pure metallic Ni face-centered cubic (fcc) crystal. XRD spectrums revealed no influence of external magnetic fields on the crystal structure of nickel. FESEM results depicts that the sample synthesized at 0 Gauss gave a yield of spherical nanoparticles, where as the sample synthesized at 800 Gauss external magnetic field gave a yield of nickel nanofibers of varying diameters and lengths. The structures synthesized at 800 G were reported to contain the maximum number of fibers per unit area. A comparative VSM analysis between sample synthesized at 800 G and the control sample (0 Gauss) was conducted which showed increase in the saturation magnetization and remnant magnetization with respect to external magnetic field. This can be attributed to magnetic shape anisotropy usually seen in 1-D nanostructures.

## References:

1. Morozov Y.G., Belousova O.V. and Kuznetsov M.V, Electric field-assisted levitation-jet aerosol synthesis of Ni/NiO nanoparticles, *Inorg. Mater.*, 2011, 47, 36-40.
2. Okawa K., Sekine M., Maeda M., Tada M., Abel M., Matsushita N., Nishio K. and Handa H., Heating ability of magnetite nanobeads with various sizes for magnetic hyperthermia at 120kHz, a noninvasive frequency, *J.Appl. Phys.*, 2006, 99, 08H102-3.
3. Kryder M. H., Magnetic thin films for data storage, *Thin Solid Films.*, 1992, 216, 174-180.
4. Chen R., Wang X., Wen H., Li L. and Gui Z., Enhancement of dielectric properties by additions of Ni nano-particles to a X7R-type barium titanate ceramic matrix, *Ceram Int.*, 2004, 30, 1271-1274.
5. Sophie G. F., Zarel V. N., Christophe T., Th L., Bernard D. and Yves C. C. J., Colossal Permittivity in Ultrafine Grain Size BaTiO<sub>3-x</sub> and Ba<sub>0.95</sub>La<sub>0.05</sub>TiO<sub>3-x</sub> Materials, *Adv Mater.* 2008, 20, 551-555.
6. Hsi C. S., Chen Y.C., Jantunen H., Wu M.J. and Lin T. C., Barium titanate based dielectric sintered with a two-stage process, *J Eur Ceram Soc.*, 2008, 28, 2581 - 2588.
7. Ganesh K. R., Ramaswamy S., Gopalakrishnan C. and John Thiruvadigal D., Effect of an external magnetic field on the morphology and magnetic properties of CoFe nanostructures, *Phys. Stat.Sol. A.*, 2011, 208, 2847-2852.
8. Chen J. Y., Liu H. R., Ahmad N., Li Y. L., Chen Z. Y., Zhou W. P. and Han X. F., Effect of external magnetic field on magnetic properties of Co-Pt nanotubes and nanowires, *J. Appl. Phys.*, 2011, 109, 07E157.
9. Liu P., Li Z., Zhao B., Yadian B. and Zhang Y., Template-free synthesis of nickel nanowires by magnetic field, *Mater Lett.*, 2009, 63, 1650- 1652.
10. Zhang M., Deng J., Zhang M. and W. Li, Shape-Controlled Synthesis of Nickel Wires Using an External Magnetic Field, *Chin. J Catal.*, 2009, 30, 447-452.
11. Sankara Narayanan T.S.N. and Seshadri S.K., Formation and characterization of borohydride reduced electroless nickel deposits, *J. Alloys Compd.*, 2004, 365, 197.
12. Wu Z. G., Munoz M. and Montero O., The Synthesis of Nickel Nanoparticles by Hydrazine Reduction, *Adv. Powder Technol.* 2010, 21, 165.
13. Ramaswamy S., Gopalakrishnan C., Kumar N.S., Littleflower A. and Ponnaivaikko M., Fabrication of Ni nanodots templated by nanoporous polysulfone membrane: Structural and Magnetic properties, *Appl. Phys. A.* 2010, 98, 481-485.
14. Chu S. Z., Wada K., Inoue S., Todoroki S., Takahashi Y. K. and Hono K., Fabrication and Characteristics of Ordered Ni Nanostructures on Glass by Anodization and Direct Current Electrodeposition, *Chem. Mater.*, 2002, 14, 4595-4602.
15. Cao H., Tie C., Xu Z., Hong J. and Sang H., Array of nickel nanowires enveloped in polyaniline nanotubules and its magnetic behavior, *Appl. Phys. Lett.* 2001, 78, 1592.
16. Ramaswamy S., Gopalakrishnan C., Ganesh K.R., Jeganathan K. and Ponnaivaikko M., Effects of argon ion bombardment on the structure and magnetic properties of ultrathin Fe films. *J. Vac. Sci. Technol. B*, 28, (2010), 795.
17. Ramaswamy S., Gopalakrishnan C. and Ponnaivaikko M., Effect of template engineering on morphology and magnetic properties of Ni nanodots fabricated using polysulfone templated lithography, *Phys. Scripta.* 2010, 82, 025603.

18. Ramaswamy S., Rajan G. K., Gopalakrishnan C. and Ponnaivaikko M., Study of magnetization reversal of uniaxial Ni nanodots by magnetic force microscopy and vibrating sample magnetometer, *J. Appl. Phys.*, 2010, 107, 09A331.
19. Lee H.H., Kuo H.T. and Chou K.S., Formation of Crystalline Nickel Fibers by Chemical Reduction in the Presence of a Magnetic Field, *J. Chin. Inst. Chem. Engrs.* 2003, 34, 327-333.
20. Sun L., Chen Q., Tang Y. and Xiong Y., Formation of one-dimensional nickel wires by chemical reduction of nickel ions under magnetic fields, *Chem. Commun.*, 2007, 27, 2844-2846.
21. Niu H., Chen Q., Ning M., Jia Y. and Wang X., Synthesis and One-Dimensional Self-Assembly of Acicular Nickel Nanocrystallites under Magnetic Fields, *J. Phys. Chem. B*, 2004, 108, 3996-3999.
22. C. Gong, L. Yu, Y. Duan, J. Tian, Z. Wu and Z. Zhang, The Fabrication and Magnetic Properties of Ni Fibers Synthesized Under External Magnetic Fields, *Eur. J. Inorg. Chem.* 18, 2008, 2884–2891.

\*\*\*\*\*